

Supplementary information for

Panorama of DNA hairpin folding observed via diffusion-decelerated fluorescence correlation spectroscopy

Yandong Yin^{a,b}, Peng Wang^{a,b}, Xin Xing Yang^{a,b}, Xun Li^{a,b}, Chuan He^{a,c,d}, Xin Sheng Zhao^{*a,b}

a) Beijing National Laboratory for Molecular Sciences and Department of Chemical Biology, College of Chemistry and Molecular Engineering; b) State Key Laboratory for Structural Chemistry of Unstable and Stable Species and Biodynamic Optical Imaging Center; and c) Synthetic and Functional Biomolecules Center; Peking University, Beijing 100871, China. d) Department of Chemistry, the University of Chicago, Chicago IL 60637, USA.

Experimental setup

The ddFCS measurements were carried out on a home-built FCS apparatus based on an inverted fluorescence microscope equipped with a temperature controller¹. A continuous-wave Ya-Ge Laser (532 nm) (SUW Tech., China) was used for illumination. The collimated laser beam was focused into the sample solution using an oil-immersion objective (100×, NA 1.4, Nikon, Japan) and kept at 20 μW before entering the objective to minimize the triplet state formation and photo bleaching. The emitted fluorescence was separated by a dichroic filter (CY3, Chroma Tech., USA) and further spectrally filtered by a bandpass 593/40 filter (Semrock, USA). After spatially filtration by a 30 μm pinhole, the fluorescence photons were divided into two channels by a non-polarizing 50/50 filter (XF121, OmegaFilters, USA). The photons were collected by two avalanche photodiodes (APDs, SPCM-AQR-14, Perkin-Elmer, USA) for the cross-correlation so as to avoid the afterpulsing in the autocorrelation². For the conventional FCS, the correlation was calculated *in situ* using a computer-implemented correlator (Flex 02-01D, [Correlator.com](http://www.correlator.com), USA). For ddFCS, the traces were recorded every 60 s. The trace with a microsphere diffusing through the confocal volume was picked out to calculate the single particle autocorrelation function (ACF). The final ddFCS curve was averaged over more than 80 ACFs to achieve a statistically stable result (Fig. S2). The sample solution was sealed between a chamber cover (GraceBio, Sigma, USA) and a cover glass which was prepared using piranha solution for more than 60 min at above 90 °C. The concentration of sample was 10 nM for the conventional FCS and 0.1% (w/v) of microspheres for ddFCS measurements, respectively.

The steady-state fluorescence experiments were carried out as previously reported³. The TMR-labeled molecules were illuminated by a continuous-wave Ya-Ge Laser (532 nm) (SUW Tech., China) and the emitted fluorescence was recorded on a Renishaw1000 microscopic spectrometer (Britain). The temperature was controlled using a THMS600 temperature controller, by

which the samples were heated from 4 to 80 °C at a speed of 2 °C per minute. The melting curves given in Fig. S7 were obtained by measuring the fluorescence intensities of TMR with the variation of temperature. The quantum yield under different temperatures was corrected by the control molecule *polyT*.

Sample preparation

The TMR-labeled single-stranded DNA sequences used in this work include hairpin *hp4* (5'-biotin-TCTCTCTCTCTCTCTCTCTTTTTT GGAA(T)₂₁TTCC-TMR-3') (Fig. S3) and control *polyT* (5'-biotin-TCTCTCTCTCTCTCTCTCTTTTTT TTTT(T)₂₁TTTT-TMR-3'). Both were purchased from Sangon Biotechnology (Shanghai, China) with HPLC purification. We took 21 nucleotides in the loop because we have been, like most researchers with a project, working on this size of the hairpin for a long time⁴⁻⁶. It has been shown that the shorter loop leads to faster association, while the dissociation rate is less affected^{5, 7, 8}. The DNA-surface interaction can influence the thermodynamic and kinetic properties, but the effect on a unimolecular reaction such as hairpin folding should be less substantial than on a bimolecular reaction such as hybridization and dehybridization of double-stranded DNA (dsDNA)⁹. In order to minimize the surface effect, we took (quite long) 24 nucleotides to link the hairpin to the microsphere besides the biotin-streptavidin conjugation. As shown in Fig. S5, little difference was seen on the kinetics of hairpin folding between free and immobilized *hp4*. However, the linker itself seems to make the hairpin slightly more stable (Fig. S7).

10 nM samples were prepared in 1×TE buffer (pH = 8.5, 10 mM Tris-HCl and 1 mM ethylene diamine tetraacetic acid (EDTA)) with 0.01% Tween 20 (Sigma, USA) before incubation with microspheres. The streptavidin-coated polystyrene microsphere (SVP-15-5, SpheroTech., USA) with diameter of 1.87 ± 0.05 μm was diluted to 0.1% (w/v) using the 1×TE buffer. The biotinylated DNA was then diluted 500-fold when it was mixed with the microsphere solution and allowed to react at 4 °C for 1 h. Free DNA molecules were washed off after centrifugation. The purified DNA attached microsphere was re-suspended in 1×TE buffer with various NaCl concentrations used in this work. We estimated that on average 50 DNA molecules were attached to each microsphere using the given properties of the microspheres (SpheroTech., USA). Trolox with a final concentration of 1 mM was introduced into the sample-microsphere complex solution as the triplet state quencher^{10, 11}.

FCS data processing and analysis

In assessing the microsphere diffusion time, the phenomenological diffusion time, τ_D , shown in Fig. 1D was obtained by fitting the ddFCS curve using the nonlinear least-squares Marquardt algorithm with the general model function²

$$G_H = \frac{1}{N} \left[1 + \left(\frac{\tau}{\tau_D} \right) \right]^{-1} \left[1 + \frac{w_0^2}{z_0^2} \left(\frac{\tau}{\tau_D} \right) \right]^{-1/2} \times \left[1 - \alpha_R + \alpha_R \exp \left(-\frac{\tau}{\tau_R} \right) \right] \quad (\text{S1})$$

where N is the average number of molecules in the confocal volume with a lateral and an axis radius of w_0 and z_0 respectively, and α_R is the fraction of molecules in non-fluorescent state caused by photo-induced processes with a lifetime of τ_R . The goodness of the fit was assessed by the R -square value, R^2 , and the fittings with $R^2 \geq 0.9$ were accepted. We wish to emphasize that the fit of the diffusion constant here is phenomenological. The microsphere diameter is bigger than the diameter of the laser focus and the dye molecules are immobilized on the surface. Therefore, the relationship between the diffusion time and the particle diameter at the limit of a very-small-sized particle no longer hold. The rotational correlation also showed up in the same time range as the translation, and it cannot be treated by a point rotor. Therefore, an accurate modeling of the translational and rotational relaxation was not attempted. Fortunately, these factors can be accurately removed.

To accurately remove the correlations other than that from hairpin folding, the procedure described in the main text was taken. The reactive correlation function $G_R(\tau)$ was normalized between $[0,1]$ and then was fitted by a double-exponential-decay function

$$(G_R(\tau) = \alpha_1 \exp(-\tau/\tau_1) + \alpha_2 \exp(-\tau/\tau_2)) \text{ or by the Maximum Entropy Method (MEM)} \\ (G_R(\tau) = \int_0^\infty \alpha(\tau_R) \exp(-\tau/\tau_R) d\tau_R), \text{ respectively.}$$

The double-exponential-decay function failed to deliver an acceptable fitting on data of all NaCl concentrations (Fig. S8). We then applied MEM for data analysis using the hybrid algorithm with nonlinear least-squares fitting¹²⁻¹⁴. We searched for both minimum of χ^2 and maximum of entropy S which are given by

$$\chi^2 = \frac{1}{M} \sum_{i=1}^M r_i^2 \quad (\text{S2})$$

$$S = - \int_0^\infty \alpha(\tau_R) \ln \alpha(\tau_R) d\tau_R \quad (\text{S3})$$

where M is the number of FCS data points and r_i is the deviation of the i th data from the fitting.

$\alpha(\tau_R)$ is the fraction of the kinetic component with relaxation time of τ_R and defined as

$\int_0^\infty \alpha(\tau_R) d\tau_R = 1$. The fraction $\alpha(\tau_R)$ shown in Fig. 3B was normalized between $[0,1]$.

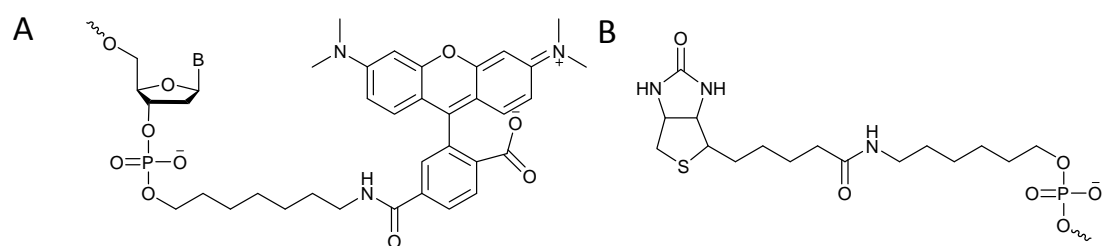


Fig. S1. Structures of TMR (A) and biotin (B) and their linkers used in this work (Sangon, China). TMR was labeled to the 3'-end of the ssDNA molecule through a C7 linker while the biotin was labeled to the 5'-end of the ssDNA molecule through a C6 linker. The wave lines stand for the DNA sequence.

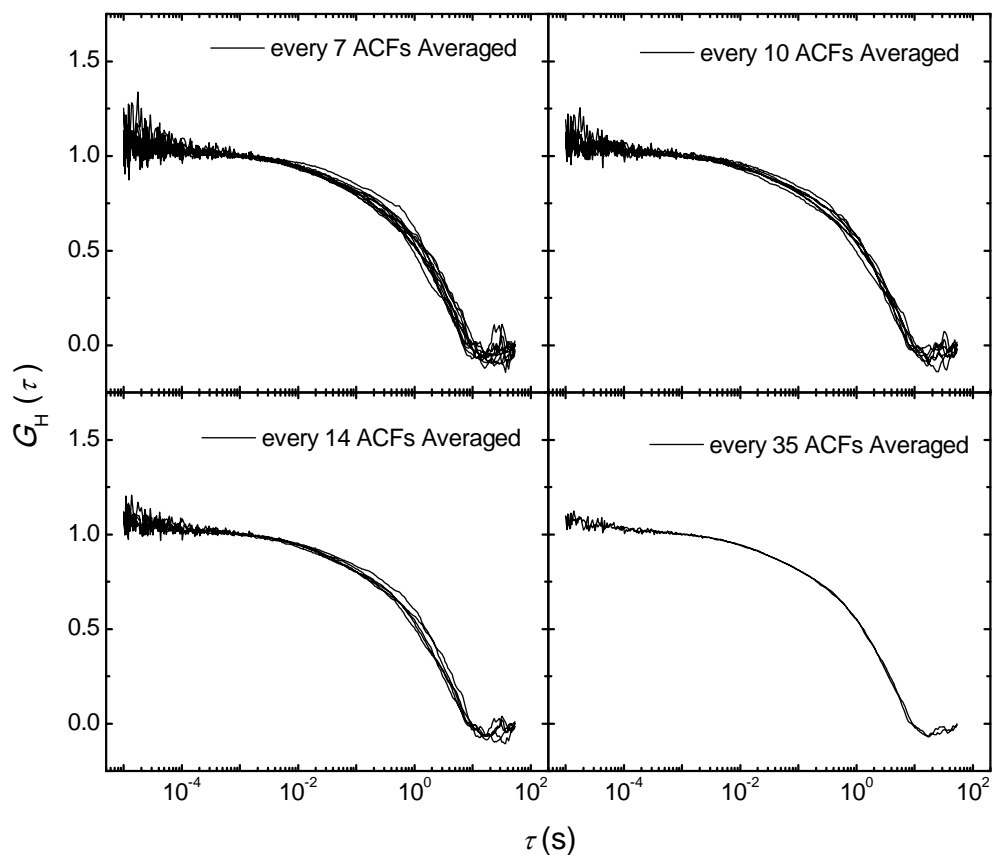


Fig. S2. Convergence of ddFCS curve over the number of individual ACFs as an average. The ddFCS data were taken on *polyT*. It is seen that ddFCS curve approaches a statistically stable result by averaging 35 ACFs. The given ddFCS curves in this work were averaged over more than 80 ACFs and were checked for reproducibility.

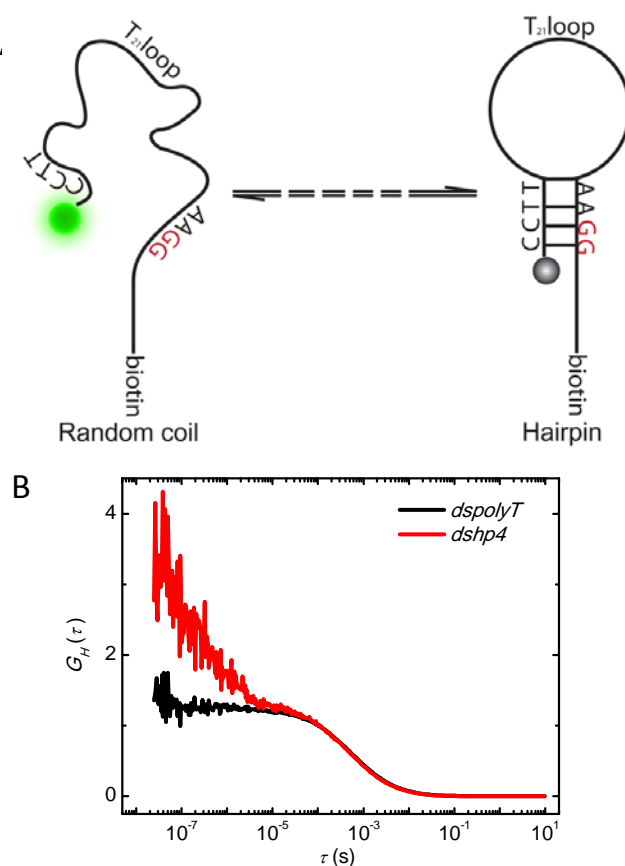


Fig. S3. A. The scheme of DNA hairpin folding of *hp4* in this work. Two dGs in the stem also acted as the fluorescence quencher, so that the conformational dynamics could be translated into the fluorescent fluctuation of the fluorescent tag (TMR). A 24-nucleotide tail labeled with biotin at the 5' end was used as a linker to the streptavidin-coated microsphere. B. To rule out the possibility that our observed relaxations in ddFCS come from TMR-DNA interaction (for example, by stacking on the end or inserting in the groove), we performed FCS experiments on dsDNAs, *dshp4* and *dspolyT*, made through the hybridization of *hp4* and *polyT* with their complementary ssDNAs, respectively. In *dshp4* the hairpin formation was inhibited, so that the relaxation processes associated with hairpin folding would disappear. Indeed, the $\sim 100\ \mu\text{s}$ relaxation does not occur in *dshp4*. The very quick relaxations seen here are due to the rotational relaxation (tens of nanoseconds in both *dshp4* and *dspolyT*) and the interaction between wobbling TMR and guanines (submicroseconds in *dshp4*). They do not disturb the kinetic measurements of hairpin folding, which occurs on a much longer time scale.

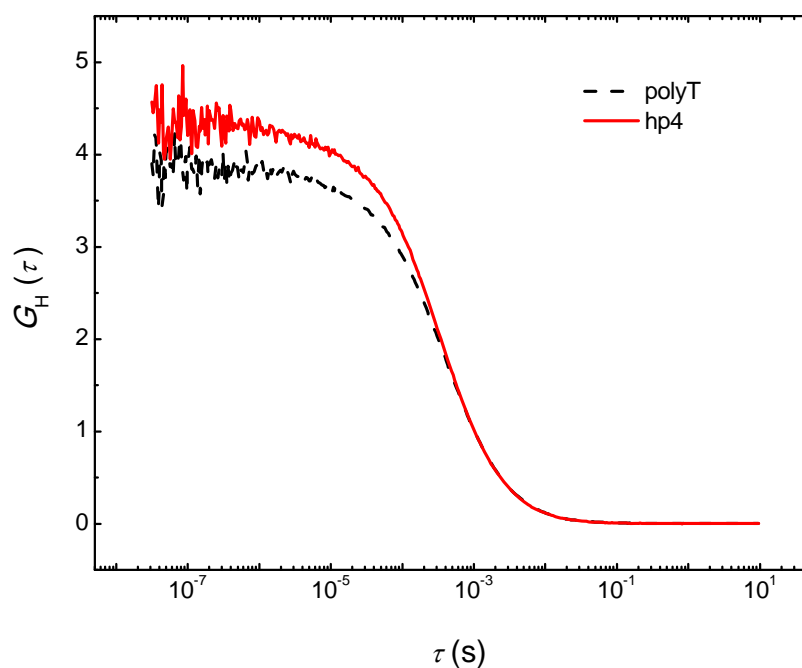


Fig. S4. The conventional FCS curves of *polyT* (dash, black) and *hp4* (solid, red). A slight difference between the DNA hairpin and control molecules was found in a time range of 1 - 10 ms. Considering that the characteristic diffusion time of *polyT* is ~0.4 ms, the fast component at about 100 μ s of the relaxation time of hairpin folding can be determined unequivocally, while the slow component longer than 1 ms cannot be identified with certainty, which led to the previous inadequate assignment of the relaxation time of hairpin folding to ~100 μ s using the conventional FCS. The experiments were carried out under 125 mM NaCl for a comparison with the ddFCS curve shown in Fig. 2.

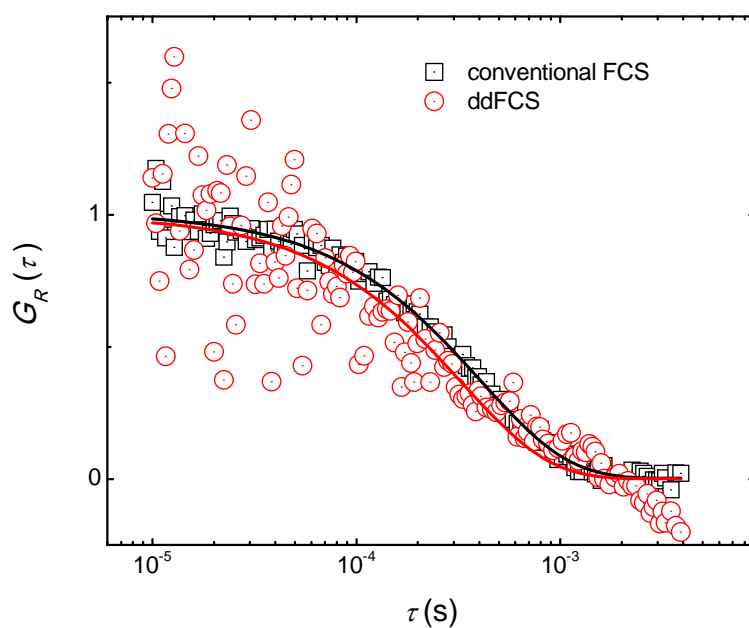


Fig. S5. Comparison of fast kinetic components (~ 0.1 ms) obtained by the conventional FCS (black) and microsphere attached ddFCS (red). Both of the measurements were carried out under 125 mM NaCl and at 20.0 ± 0.5 °C. The little difference between the kinetic relaxations revealed by the two FCS assays suggests that the immobilization of the DNA molecules with the microsphere through our biotin-streptavidin conjugation had little influence on the kinetics of hairpin folding.

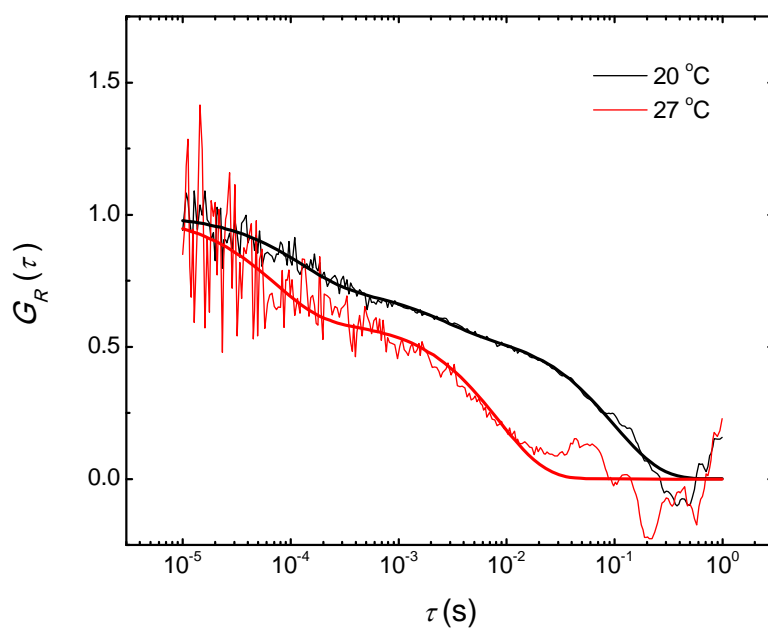


Fig. S6. Correlation data, G_R , of hairpin folding obtained by ddFCS assay at $20.0 \pm 0.5^\circ\text{C}$ (black) and $27.0 \pm 0.5^\circ\text{C}$ (red), respectively. The higher temperature resulted in a faster hairpin folding as compared to the lower temperature. The experiments were carried out under 200 mM NaCl.

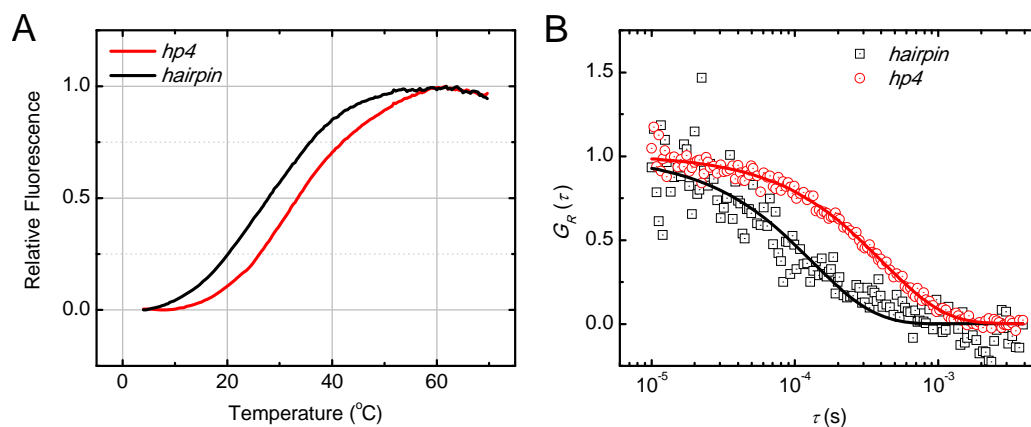


Fig. S7. Comparison of thermodynamic and kinetic features between a hairpin molecule (black) and that with an ssDNA tail, which in this work was used to link the DNA molecule to the microsphere (red). *hp4* is the hairpin molecule with a tail used in this work, and *hairpin* stands for the hairpin molecule without the linker tail (5'-GGAATTTTTTTTTTTTTTTTTTTTTTCC-TMR-3'). A. The melting curves taken under 1 M NaCl suggest that the existence of the ssDNA tail stabilizes the stem structure of the hairpin molecule. B. The correlation data, G_R , obtained by the conventional FCS experiments under 125 mM NaCl indicate that the hairpin molecule containing an ssDNA tail exhibits a slower partial folding, in agreement with what the melting curves suggest.

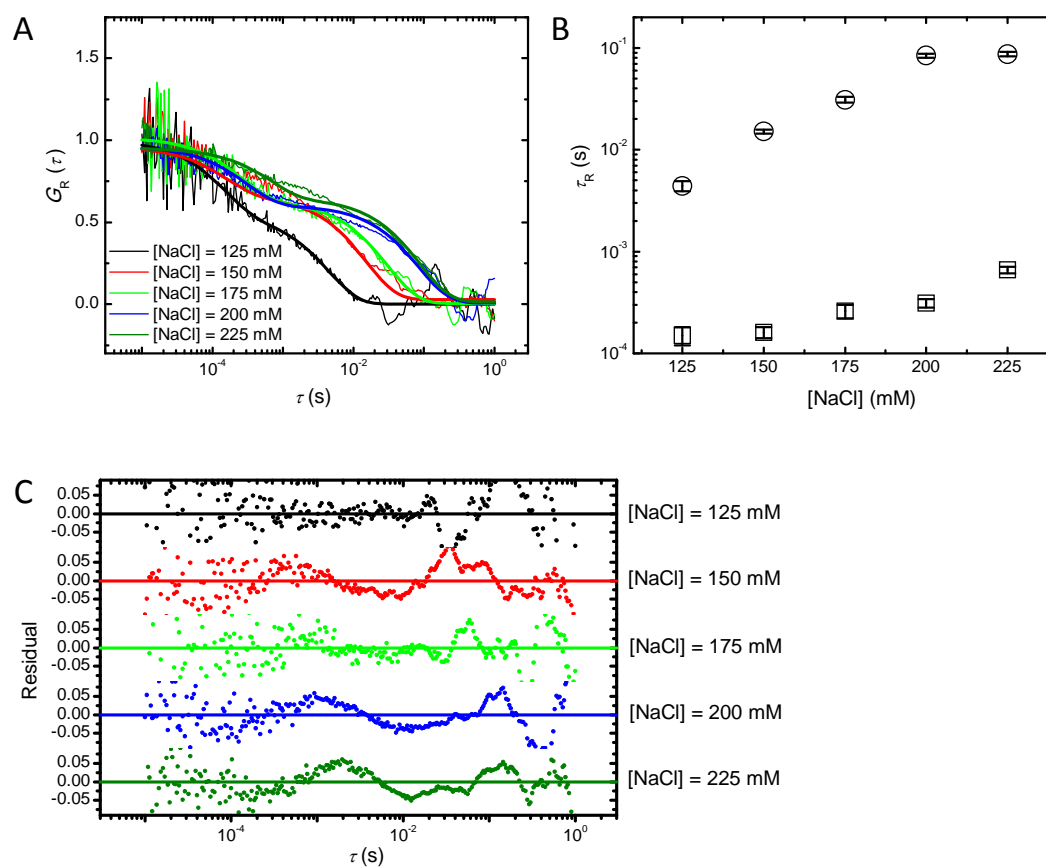


Fig. S8. (A) ddFCS curves of hairpin folding under different NaCl concentrations and corresponding fittings using double-exponential-decay function. (B) Relaxation time of both fast process (open square) and slow process (open circle) fitted from (A) as function of NaCl concentration. The NaCl concentration significantly influences the slow process whereas the fast process is less affected. (C) Residuals of the double-exponential fit in (A).

References

1. X. Chen, Y. Zhou, P. Qu and X. S. Zhao, *J. Am. Chem. Soc.*, 2008, **130**, 16947-16952.
2. O. Krichevsky and G. Bonnet, *Rep. Prog. Phys.*, 2002, **65**, 251-297.
3. C. Chen, W. Wang, Z. Wang, F. Wei and X. S. Zhao, *Nucleic Acids Res.*, 2007, **35**, 2875-2884.
4. F. Wei, C. Chen, L. Zhai, N. Zhang and X. S. Zhao, *J. Am. Chem. Soc.*, 2005, **127**, 5306-5307.
5. G. Bonnet, O. Krichevsky and A. Libchaber, *Proc. Natl. Acad. Sci. U.S.A.*, 1998, **95**, 8602-8606.
6. J. Jung and A. Van Orden, *J. Am. Chem. Soc.*, 2006, **128**, 1240-1249.
7. P. Qu, X. Yang, X. Li, X. Zhou and X. S. Zhao, *J. Phys. Chem. B*, 2010, **114**, 8235-8243.
8. W. Zhang and S. J. Chen, *Biophys. J.*, 2006, **90**, 778-787.
9. C. Chen, W. Wang, J. Ge and X. S. Zhao, *Nucleic Acids Res.*, 2009, **37**, 3756-3765.
10. I. Rasnik, S. A. McKinney and T. Ha, *Nat. Methods*, 2006, **3**, 891-893.
11. Campos L. A., J. Liu, X. Wang, Ramanathan R., D. S. English and V. Muñoz, *Nat. Methods*, 2011, **8**, 143-146.
12. P. J. Steinbach, R. Ionescu and C. R. Matthews, *Biophys. J.*, 2002, **82**, 2244-2255.
13. P. J. Steinbach, *J. Chem. Inf. Comput. Sci.*, 2002, **42**, 1476-1478.
14. Y. Yin, X. Zhou and X. S. Zhao, *Acta Phys. Chim. Sin.*, 2010, **26**, 1087-1092.